Analytic estimation of line edge roughness for large-scale uniform patterns in electron-beam lithography

Rui Guo and Soo-Young LeeJin Choi, Seom-Beom Kim, Sung-Hoon Park, In-Kyun Shin, and Chan-Uk Jeon

Citation: J. Vac. Sci. Technol. B **34**, 06K605 (2016); doi: 10.1116/1.4968186
View online: http://dx.doi.org/10.1116/1.4968186
View Table of Contents: http://avs.scitation.org/toc/jvb/34/6
Published by the American Vacuum Society

Analytic estimation of line edge roughness for large-scale uniform patterns in electron-beam lithography

Rui Guo and Soo-Young Lee[a)]
Department of Electrical and Computer Engineering, Auburn University, Auburn, Alabama 36849

Jin Choi, Seom-Beom Kim, Sung-Hoon Park, In-Kyun Shin, and Chan-Uk Jeon
Samsung Electronics, Mask Development Team, 16 Banwol-Dong, Hwasung, Kyunggi-Do 445-701, South Korea

(Received 5 July 2016; accepted 8 November 2016; published 22 November 2016)

As the feature size continues to be reduced well below nanoscale, the line edge roughness (LER) will eventually become a resolution-limiting factor in the electron-beam (e-beam) lithography since the LER does not scale with the feature size. Therefore, to achieve the highest resolution possible by the e-beam lithography, the LER needs to be minimized. A simulation-based or experimental approach for estimating and minimizing the LER normally requires a great deal of effort to analyze the relationship between the LER and e-beam parameters and thus is time-consuming. Previously, an analytic method for estimating and minimizing the LER was developed for the case of a single line. In this paper, an extension of the estimation method for large-scale uniform patterns is described. In a large pattern, the exposure distribution over a feature varies with the location within the pattern, and the location dependency is due to the global exposure. The analytic expression of LER derived for a single line is adjusted depending on the location. The amount of adjustment for each of the critical locations is determined by the stochastic information on the global exposure at that location. The LER at a location is obtained through an interpolation using the LERs at the critical locations. The LER evaluated by the analytic expression of LER has been compared with that obtained through simulation. [http://dx.doi.org/10.1116/1.4968186]

I. INTRODUCTION

Electron-beam (e-beam) lithography plays an important role in nanofabrication, being able to transfer high-resolution patterns onto the resist.[1–4] However, for a circuit pattern of nanoscale features, the proximity effect and the line edge roughness (LER) put a fundamental limit on the minimum feature size and maximum circuit density that can be realized.[5] Various effective and efficient schemes for correcting the proximity effect were developed by many researchers.[6–9] For minimizing the LER, many of the previous efforts were based on an empirical or trial-and-error approach via experiment or simulation.[10–12] However, such a method can be very time-consuming and costly since repetitive simulations or experiments may be required. In order to avoid the simulation and experiment, one may take an analytic approach to estimating and minimizing the LER. In the efforts to estimate the effects of the LER on the device behaviors,[13,14] theoretical models were formulated; however, an analytic expression of the LER was not derived.

In our previous study,[15] a new analytic method for estimating the LER at any layer of resist was developed for the case where a long single line is exposed with a uniform dose. Without having to obtain the remaining resist profile, the analytic (mathematical) expression of LER is derived explicitly from the stochastic fluctuation of the developing rate distribution on which the remaining resist profile mainly depends. Also, an analytic procedure for minimizing the LER with respect to the dose was developed with all the other e-beam lithographic parameters, i.e., beam energy, developing time, etc., fixed.

In general, it is not straightforward to apply the single-line result of LER expression to a large circuit pattern since the exposure (energy deposited in the resist) level varies with the location within the pattern. However, for a large uniform pattern such as line-space (L/S) patterns where the same feature is replicated uniformly, the exposure level varies gradually in space. Note that the spatial variation of exposure level mainly depends on the global exposure. Therefore, it is possible to derive the LER analytically by adjusting the LER expression for a single line according to the location in a large uniform pattern. The analytic expression of LER is derived at three critical locations, i.e., center, edge, and corner (see Fig. 1), by modeling the difference of the stochastic exposure distribution between the locations and incorporating it into the single-line result. The LER at other locations may be obtained through an interpolation using the LERs at the critical locations.

A specific goal of this study is to obtain an explicit analytic expression of LER which can be used for minimization of LER later. In order to achieve the goal, in some steps of derivation, certain assumptions and approximations are made. Therefore, it needs to be pointed out that the derivation of LER described in this paper is not completely analytic.

The rest of the paper is organized as follows. The exposure and development models are described in Sec. II. The derivation for the LER of a single line is briefly reviewed in Sec. III. The procedure for estimating the LER for a large uniform pattern is described in Sec. IV. The results of estimating the LER

[a)]Electronic mail: leesooy@eng.auburn.edu

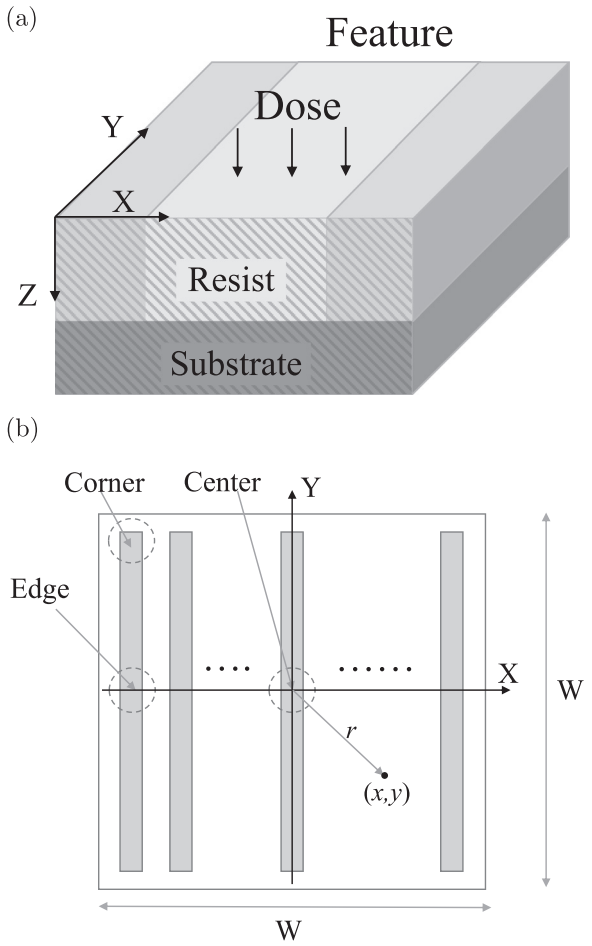

FIG. 1. (a) 3D model of substrate system, where a line is exposed with a uniform dose and (b) a large-scale uniform pattern with line features where the three critical regions (corner, edge, and center) are shown. The size of the pattern is $W \times W$.

at the critical locations are discussed in Sec. V, followed by a summary in Sec. VI.

II. MODELS

In this section, the modeling of the e-beam lithographic process and the assumptions made in the modeling are described.

A. Exposure model

A three-dimensional (3D) model of substrate system is employed in this study. As shown in Fig. 1(a), a resist layer is on the top of the substrate where the X-Y plane corresponds to the top surface of resist, and the resist depth is along Z-dimension. A large-scale uniform pattern considered in this study is illustrated in Fig. 1(b), where the three critical locations, corner, edge, and center, are shown. The 3D point spread function (PSF) is denoted by $psf(x,y,z)$ (see Fig. 2), which describes the exposure distribution in the resist when a point on the X-Y plane is exposed. Let the e-beam dose distribution on the surface of resist be denoted by $D(x, y)$ and the exposure at the point (x, y, z) in the resist by $e(x,y,z)$. Then, the 3D spatial distribution of exposure can be expressed by the following convolution:

$$e(x,y,z) = \int\int D(x-x', y-y')psf(x',y',z)dx'dy'. \quad (1)$$

The exposure $e(x,y,z)$ is stochastic since the PSF $psf(x,y,z)$ is stochastic. For a uniform substrate and a stable e-beam tool, the stochastic properties of PSF must be space-invariant. That is, the mean and variance of PSF (see Fig. 2), denoted as $m_{psf}(x,y,z)$ and $\sigma^2_{psf}(x,y,z)$, respectively, are space-invariant. Then, the mean exposure, $m_e(x,y,z)$, can be expressed as

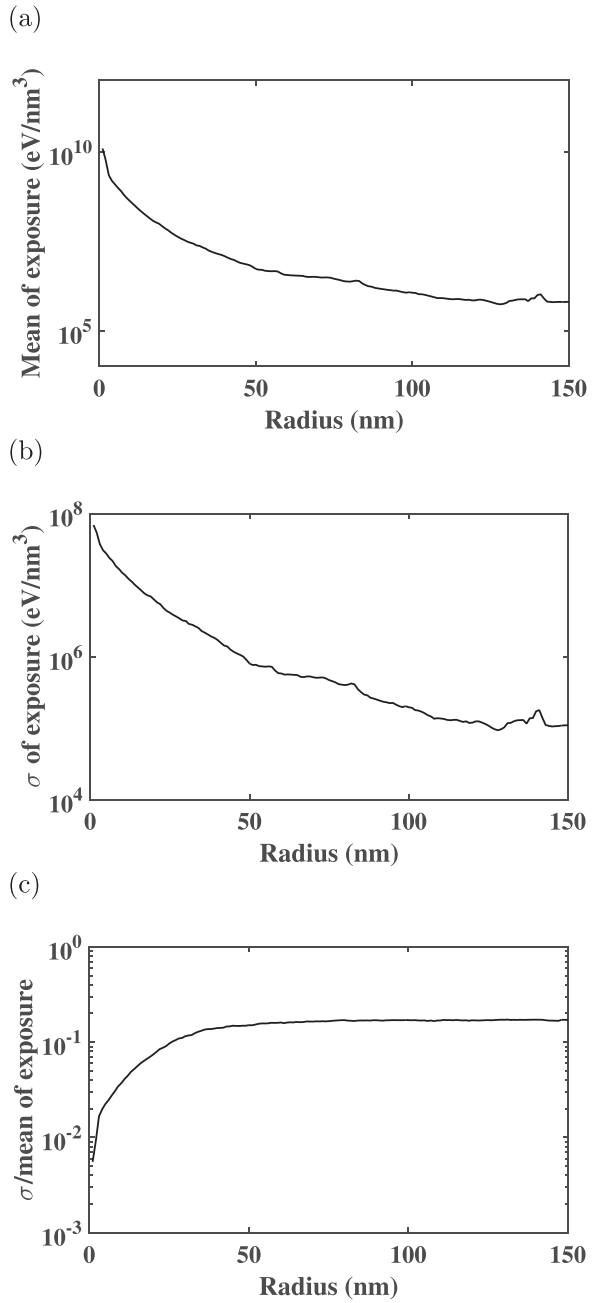

Figure 2

FIG. 2. Moments of stochastic PSF generated by CASINO Monte Carlo simulation: 300 nm PMMA on Si, dose of 640 $\mu C/cm^2$, and beam energy of 50 keV: (a) mean, (b) standard deviation, and (c) ratio of standard deviation/mean.

$$m_e(x,y,z) = \int\int D(x-x',y-y')m_{psf}(x',y',z)dx'dy'. \quad (2)$$

Also, assuming that $psf(x,y,z)$ and $psf(x',y',z)$ are uncorrelated, the variance of exposure, $\sigma_e^2(x,y,z)$, can be derived as

$$\sigma_e^2(x,y,z) = \int\int D(x-x',y-y')\sigma_{psf}^2(x',y',z)dx'dy'. \quad (3)$$

B. Development model

The resist layer is partitioned into cubic cells, and the stochastic exposure is estimated at each cell. Then the stochastic developing rate $R(x,y,z)$ of each cell is calculated from its corresponding exposure $e(x,y,z)$ through a nonlinear exposure-to-rate conversion formula, which may be experimentally determined. Given a spatial distribution of the developing rate, the remaining resist profile is determined through the resist development process. Assume that the resist development process can be modeled by "development paths" where a development path is defined as a path along which the resist is developed, as illustrated in Fig. 3. Each development path starts from the resist surface and goes toward the boundary of resist profile. Given a possible edge location x, its development path is the path that takes the developing time (on average) to reach the location from the top surface of resist, and its length is denoted by s. Note that the LER is proportional to the length fluctuation of the development path of an edge location. The developing rate along the development path is expressed by $R(p)$, where $0 \le p \le s$, as shown in Fig. 3. The analytic expression of LER is derived utilizing the concept of development path later.

III. LER FOR SINGLE LINE

In this section, our previous work[15] on the analytic derivation of LER for a single line is briefly reviewed.

The LER is defined as the variation of the edge location at a layer (i.e., the X-Y plane at a given depth into the resist) of the remaining resist profile as shown in Fig. 3, and is quantified as the standard deviation of the edge location x measured in the lateral dimension given a developing time T, i.e.,

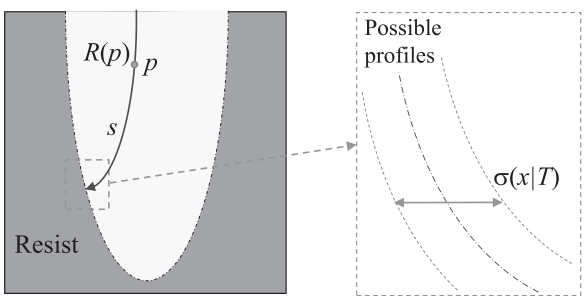

FIG. 3. Development path in the resist and the variation $[\sigma(x|T)]$ of edge location with a fixed developing time. Note that $p=0$ and $p=s$ correspond to the starting and ending points of a development path, respectively. $R(p)$ is the developing rate at p.

$$\text{LER} = \sigma(x|T). \quad (4)$$

Assuming that all the stochastic information on the developing rate distribution for a single line is given, i.e., generated from a set of the stochastic developing-rate distributions $R(x,y,z)$ obtained from the Monte Carlo simulation, the derivation of an analytic expression of the LER is carried out in three steps: (1) given an edge location x_0 at a layer (z_0), at which the LER is to be estimated, find the development path to reach the location and derive the fluctuation of the developing time T taken by the development path, (2) estimate the direction of the development path at the edge location x_0, and (3) derive the expression of the LER given a developing time T.

Since the developing process is isotropic, it is not easy to derive the development path analytically in one step, and therefore, an iterative method is used to derive the development path.[15] The fluctuation of developing time can be directly derived from the developing-rate distribution along the development path. The developing time T is expressed as the integral of $1/R(p)$ along the development path

$$T = \int_{p=0}^{s} \frac{dp}{R(p)}. \quad (5)$$

Assuming that the correlation of $1/R(p)$ at any two points (p_1, p_2) on the development path denoted as $Cov_{1/R}(p_1,p_2)$ is known, i.e., the stochastic information can be extracted from a set of stochastic developing-rate distributions generated from the Monte Carlo simulation, the variance of developing time is derived as

$$\sigma^2(T|s) = \int_{p=0}^{s} \sigma_{\frac{1}{R}}^2(p)dp + \int_{p_1=0}^{s}\int_{p_2=0}^{s} Cov_{\frac{1}{R}}(p_1,p_2)dp_2dp_1. \quad (6)$$

The fluctuation of the development-path length (s given T) may be related to the fluctuation of developing time taken by this path. If the developing rate around s is represented by the mean of developing rate at s, i.e., $m_R(s)$, the fluctuation of developing time can be directly converted into the fluctuation of s given T as

$$\sigma(s|T) = \sigma(T|s) \cdot m_R(s). \quad (7)$$

Since the LER is measured in the lateral dimension (X-dimension), $\sigma(s|T)$, which is derived along the direction of developing path, needs to be projected onto the X-dimension to get the LER (see Fig. 4)

$$\sigma(x|T) = \frac{\sigma(T|s) \cdot m_R(s)}{\cos(\theta)}. \quad (8)$$

It needs to be pointed out that the interaction between adjacent development paths is not taken into account in the above derivation. The interaction tends to decrease the variation (of path length) among the paths and reduces the LER. Therefore, an adjustment factor[16] is employed to compensate the interaction between paths, and the final expression of LER [from Eqs. (6) and (8)] is given as

$$\mathrm{LER}(x|T) = \sigma(x|T) = \frac{\rho_T(s)+1}{2} \cdot \frac{\sqrt{\left(\int_{p=0}^{s} \sigma^2_{\frac{1}{R}}(p)dp + \int_{p_1=0}^{s}\int_{p_2=0}^{s} Cov_{\frac{1}{R}}(p_1,p_2)dp_2dp_1\right)} \cdot m_R(s)}{\cos(\theta)}. \tag{9}$$

Note that, in this equation, $\rho_T(s)$ involves the covariance of $1/R$ between two adjacent paths interacting during the resist development process while $Cov_{1/R}(p_1,p_2)$ is the covariance of $1/R$ between two points on a path.

IV. LER FOR LARGE-SCALE PATTERN

The exposure level in a large pattern significantly varies with the location due to the proximity effect, and therefore, the LER is also location-dependent. Given a location in such a pattern, it is possible to use the analytic expression of LER derived for a single line by computing the stochastic properties of exposure at the location. However, this approach requires a repetitive work of computing the exposure distribution at each location. In this study, the LER expression for a single line is adjusted by considering the location dependency of exposure. In a large pattern, the exposure at a location may be decomposed into "local" and "global" exposures where the former refers to the exposure contribution from the forward-scattering of electrons and the latter to that from the back-scattering. The exposure distribution in the case of a single line is mainly of local exposure. Therefore, the difference in the exposure distribution between a single line and a large pattern is due to the global exposure which varies significantly with the location, e.g., the center, edge, and corner, as shown in Fig. 5. The adjustment of the analytic expression of LER for a single line is done according to the distribution of the global exposure.

A. Modeling of global exposure

Let the back-scattering part of a PSF be denoted by psf_B, which spatially varies slow as shown in Fig. 2. Therefore, the mean and variance of psf_B can be approximated as

$$m_{psf_B}(r) = \begin{cases} M_B & \text{when} \quad r \le r_0 \\ 0 & \text{when} \quad r > r_0 \end{cases}$$
$$\sigma^2_{psf_B}(r) = \begin{cases} V_B & \text{when} \quad r \le r_0 \\ 0 & \text{when} \quad r > r_0, \end{cases} \tag{10}$$

where r_0 is the radius of the PSF domain, and $r = \sqrt{x^2+y^2}$.

M_B and V_B are derived by the average mean and variance of the backscattering part of PSF within the PSF domain, respectively. An example of this approximation is shown in Fig. 6, where r_0 is 20 μm.

In the case of a large uniform pattern, the global exposure may be computed without performing the feature-by-feature convolution. The entire pattern is considered to be a single feature of the same size $W \times W$, where the effective dose is the actual dose scaled by the feature density d [$d = 0.5$ when L = S in a L/S pattern as illustrated in Fig. 1(b)]. Then, computing the global exposure at a point is equivalent to finding the overlapped area between the pattern and the domain of a PSF centered at the point. From Eq. (1), the global exposure e_G can be computed by

$$e_G(x,y,z) = \int_{x'=-\frac{W}{2}}^{\frac{W}{2}} \int_{y'=-\frac{W}{2}}^{\frac{W}{2}} d \cdot psf_B(x-x', y-y', z)dx'dy'. \tag{11}$$

The fluctuation of the global exposure $\sigma^2_{e_G}$, which affects the LER, can be derived from Eqs. (10) and (11) through the same procedure as in Eq. (3).

$$\sigma^2_{e_G}(x,y) = \begin{cases} V_B d\pi r_0^2 & \text{when} \quad r < \frac{W}{2} - r_0 \\ \left(\frac{1}{2}\sin\theta_1 \cdot \left(\frac{W}{2}-|x|\right)r_0 + \frac{1}{2}\sin\theta_2 \cdot \left(\frac{W}{2}-|y|\right)r_0 + \left(\frac{W}{2}-|x|\right)\left(\frac{W}{2}-|y|\right) + \frac{1}{2}\left(\frac{3\pi}{2}-\theta_1-\theta_2\right)\right) V_B d & \text{when} \quad r \ge \frac{W}{2} - r_0, \end{cases} \tag{12}$$

where

$$\theta_1 = \cos^{-1}\left(\frac{\frac{W}{2}-|x|}{r_0}\right),$$
$$\theta_2 = \cos^{-1}\left(\frac{\frac{W}{2}-|y|}{r_0}\right). \tag{13}$$

B. Relationship between global exposure and LER

The LER at a location may be modeled by two parts: the contribution from the local exposure, which is independent of the location, and the contribution from the global exposure. The exposure distribution in the case of a single line is mainly of local exposure, and therefore, the LER derived for a single line [Eq. (9)] may approximate the LER contribution from the local exposure in a large pattern.

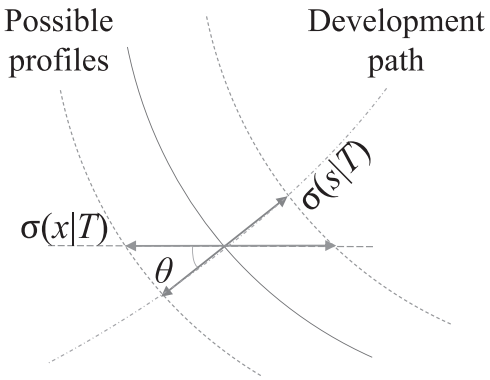

FIG. 4. Fluctuation of the development-path length [$\sigma(s|T)$] is projected onto the X (lateral) dimension [$\sigma(x|T)$]. The direction of the development path is perpendicular to the possible profiles.

Given a location at which the LER is to be estimated, the location is referred to by the variable r for computing the global exposure as in Sec. IV A and by the variable x_l for expressing the edge location in the local coordinate (see Fig. 7), to be distinguished from the global variable x. The x_l represents the relative location of edge with respect to the target edge location of a feature. That is, $x_l = 0$, $x_l < 0$, and $x_l > 0$ correspond to the cases where the actual edge is on the target location, inside the feature, and outside the feature, respectively. In the case of a single line, x_l is the same as x in Eq. (9). It should be mentioned that x_l is only an auxiliary variable, not independent of x.

Let $\Delta\mathrm{LER}(x_l|T,(x,y))$ denote any change of the LER due to the global exposure, compared to the LER for a single line. The fluctuation in the global exposure is relatively small compared to that in the (total) exposure and does not vary substantially within a small region. Also, the LER tends to increase as the exposure fluctuation increases. Therefore, $\Delta\mathrm{LER}(x_l|T,(x,y))$ may be approximated to be linearly proportional to the added exposure fluctuation $\sigma_{e_G}(x,y)$ (from the global exposure)

$$\Delta\mathrm{LER}(x_l|T,(x,y)) = \alpha\cdot\sigma_{e_G}(x,y), \tag{14}$$

where α is a positive proportional constant (change rate).

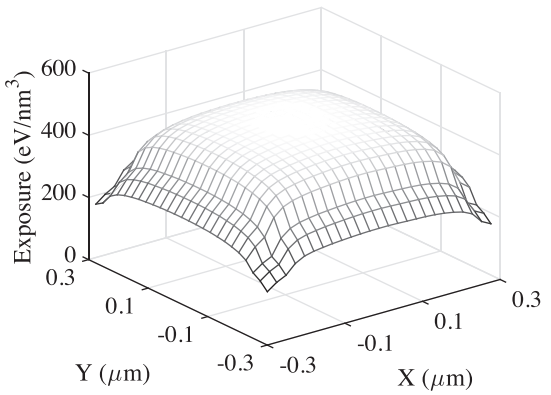

FIG. 5. Global exposure distribution in a large-scale uniform pattern: 300 nm PMMA on Si, dose of 640 μC/cm^2, and beam energy of 50 keV.

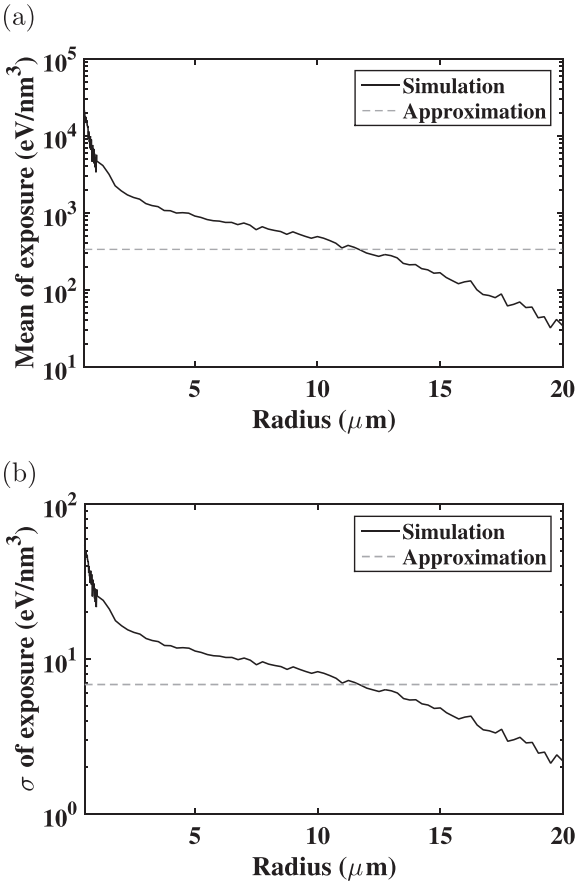

FIG. 6. Approximated (a) mean, M_B, and (b) standard deviation, V_B, of the back-scattering part of a PSF obtained from the Monte Carlo simulation: 300 nm PMMA on Si, dose of 640 μC/cm^2, and beam energy of 50 keV. M_B and V_B are indicated by the dashed lines.

The proportional constant α may be found using the LER for a single line, denoted by $\mathrm{LER}_{\mathrm{single}}(x_l|T)$, where $\sigma_{e_G}=0$ and the LER at the center of a pattern, $\mathrm{LER}_{\mathrm{cent}}(x_l|T)$, where $\sigma_{e_G}(0)=\sqrt{V_B d\pi r_0^2}$ [see Eq. (12)]. The LER at the center can be derived by the same method for a single line, but with the distribution of developing rate in the center region. Then, α is expressed as

$$\alpha = \frac{\mathrm{LER}_{\mathrm{cent}}(x_l|T) - \mathrm{LER}_{\mathrm{single}}(x_l|T)}{\sqrt{V_B d\pi r_0^2}}. \tag{15}$$

And the LER at a (x, y) can be derived as

$$\mathrm{LER}(x_l|T,(x,y)) = \Delta\mathrm{LER}(x_l|T,(x,y)) + \mathrm{LER}_{\mathrm{single}}(x_l|T) \tag{16}$$

$$= \frac{\left(\mathrm{LER}_{\mathrm{cent}}(x_l|T) - \mathrm{LER}_{\mathrm{single}}(x_l|T)\right)\sigma_{e_G}(x,y)}{\sqrt{V_B d\pi r_0^2}} + \mathrm{LER}_{\mathrm{single}}(x_l|T). \tag{17}$$

The exposure contrast over a feature edge also affects the LER. A larger exposure contrast tends to lead to a smaller LER since the room for variation among neighboring edge locations becomes smaller when the exposure decreases faster (over the edge). Therefore, this inverse relationship

between the LER and exposure contrast is approximated to be linear. Then, the LER expression may be further adjusted according to the location-dependent exposure contrast. The exposure contrast $C(x, y)$ is quantified as the exposure difference from the center of a feature to the middle point between features. An example of the location dependency of the exposure contrast is provided in Fig. 8.

Finally, the LER is expressed as follows:

$$\mathrm{LER}\left(x_l|T,(x,y)\right) = \left(\frac{\left(\mathrm{LER}_{\mathrm{cent}}(x_l|T) - \mathrm{LER}_{\mathrm{single}}(x_l|T)\right)\sigma_{eG}(x,y)}{\sqrt{V_B d\pi r_0^2}} + \mathrm{LER}_{\mathrm{single}}(x_l|T)\right)\frac{C_{\mathrm{single}}}{C(x,y)}, \tag{18}$$

where C_{single} is the exposure contrast in the case of a single line.

Given a location (x, y) in a large pattern, the effects of the global-exposure fluctuation and the exposure contrast on the LER are determined, and the LER is expressed as a function of the local variable x_l derived from x.

V. RESULTS AND DISCUSSION

In order to verify the accuracy of the proposed analytic method, its results are compared with those obtained through the simulation. A typical substrate system is employed, where a resist layer of PMMA with a certain thickness is on the top of the Si substrate. A large L/S pattern of size $50 \times 50\mu$m is exposed with a uniform dose.

For the simulation, a set of stochastic PSFs is generated using two Monte Carlo simulation programs, the CASINO and SEEL,[9] where the beam diameter is set to 3 nm. The dose level is controlled by the number of electrons. The stochastic exposure distribution in the resist is computed through the convolution of stochastic PSFs and the dose distribution in the pattern [see Eq. (1)]. The exposure is converted into the stochastic developing-rate distribution through a nonlinear mapping function determined from the experiment.[17] Then, a development simulation is carried out using the path-based method developed earlier,[17] to obtain the remaining resist profile. The process of development simulation continues until the resist profile reaches a certain edge location (x_l) at which the LER is to be evaluated (see Fig. 7).

While the proposed analytic method can be applied to any layer of resist, the results for the bottom layer are provided in this paper since the LER is usually largest at the bottom layer. The LER estimated by computation from the analytic expression is compared with that obtained by the simulation for varying edge location x_l, where $x_l = 0$ corresponds to the target edge location (see Fig. 7). The edge location is controlled by changing the developing time with the same exposure (developing rate) distribution (see Fig. 7).

In Fig. 9, the results for a L/S pattern with the line width of 100 nm are provided at the three critical regions, the corner, edge, and center. The beam energy is 50 keV, the resist thickness is 300 nm, and the dose level is $64\mu\mathrm{C/cm}^2$. Note that the developing time is different for the same edge location in a different region since the exposure distribution varies with location. It can be seen that the LER estimated

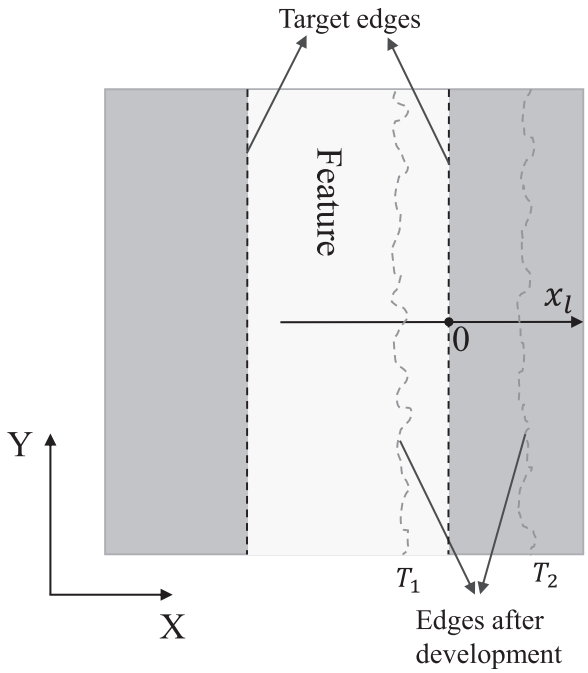

FIG. 7. Local variable x_l is defined with respect to the target edge of feature. After the development process, the boundary (edge) of remaining resist profile can be inside ($x_l < 0$) or outside ($x_l > 0$) the feature. For example, the two dashed curves represent the two possible boundaries for two different developing times, T_1 and T_2 where $T_1 < T_2$.

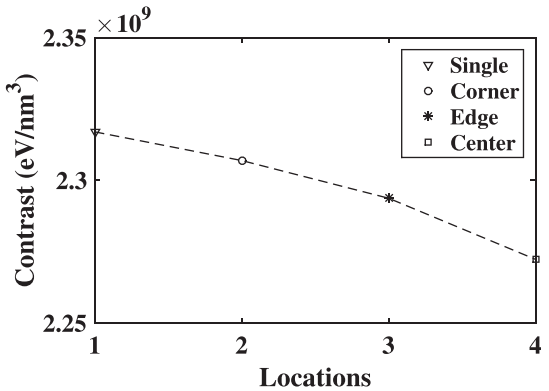

FIG. 8. Location dependency of exposure contrast: line width of 100, 300 nm PMMA on Si, beam energy of 50 keV, and dose of 64 $\mu\mathrm{C/cm}^2$. The exposure contrast for a single line is also shown.

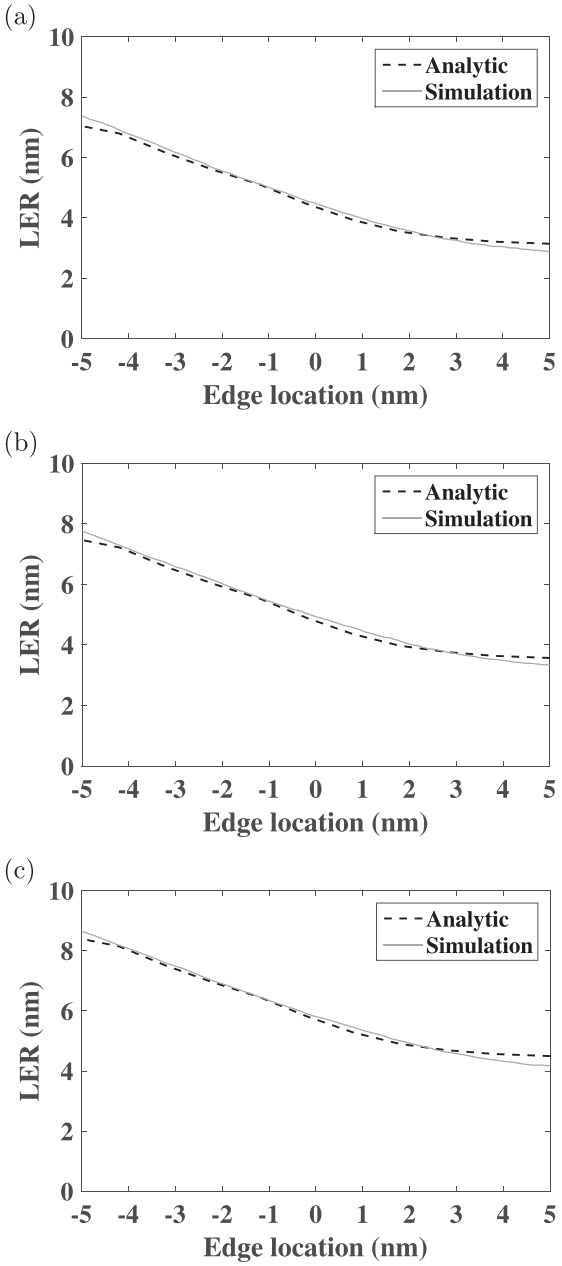

FIG. 9. LER estimated by the analytic and simulation methods at (a) corner, (b) edge, and (c) center: line width of 100 nm, 300 nm PMMA on Si, beam energy of 50 keV, and dose of 64 $\mu C/cm^2$.

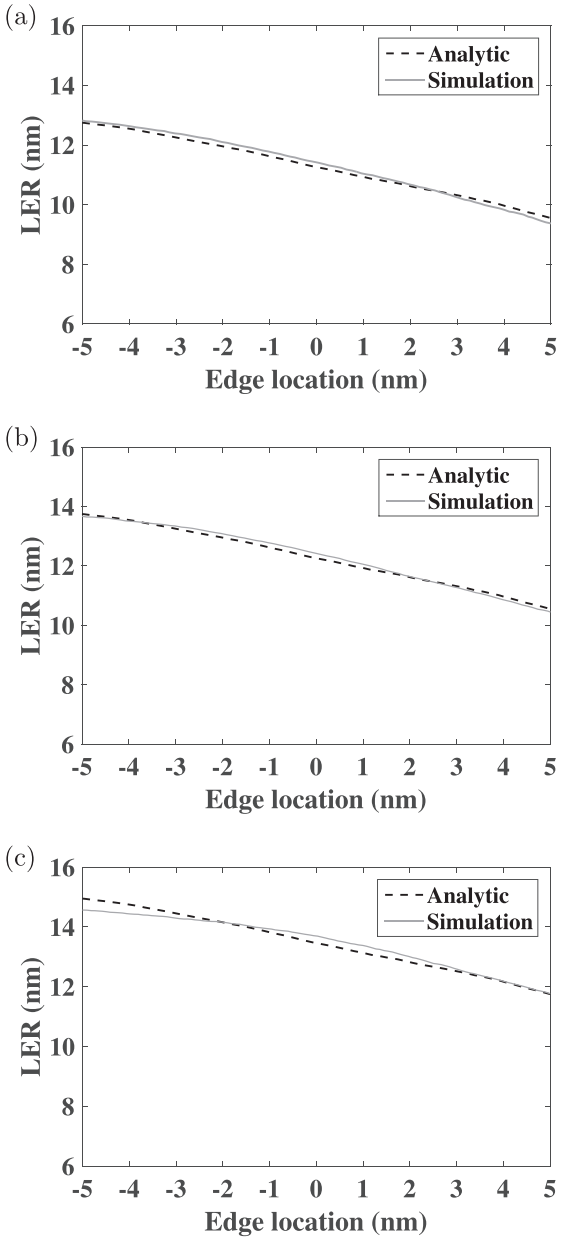

FIG. 10. LER estimated by the analytic and simulation methods at (a) corner, (b) edge, and (c) center: line width of 50 nm, 500 nm PMMA on Si, beam energy of 50 keV, and dose of 64 $\mu C/cm^2$.

by the analytic method is well matched with that by the simulation method. In Fig. 10, the results for a narrower line width of 50 nm and a larger resist thickness of 500 nm are provided with the dose level of $64\mu C/cm^2$ and the beam energy of 50 keV. A similar observation, i.e., a close match between the analytic and simulation results, can be made.

One observation to be made is that the behavior of LER with the edge location varied (i.e., the shape of LER curve) does not change substantially with the location within a pattern. This is due to the fact that the spatial distribution of exposure cross a line feature has a similar shape independent of the location though the exposure level varies with the location. Note that the shape of exposure distribution mainly depends on the local exposure. Another observation is that the LER is largest at the center and decreases toward the corner. Both the exposure fluctuation and contrast affect the LER. A larger fluctuation tends to lead to a larger LER while a higher contrast to a smaller LER. However, in the cases in Figs. 9 and 10, the (absolute) exposure fluctuation, which is largest at the center, is dominant. Also, it is seen that the LER is larger in Fig. 10 than in Fig. 9. A reason for this result is that the exposure contrast over the feature boundary, to which the LER is inversely proportional, is lower for a thicker resist at the bottom layer and also for a narrower gap between lines. Another reason is that the development path to the bottom layer is longer for a thicker resist and the LER tends to be larger when edges are reached through longer development paths.

The LER at locations other than the three critical locations can be computed through an interpolation of the LER's

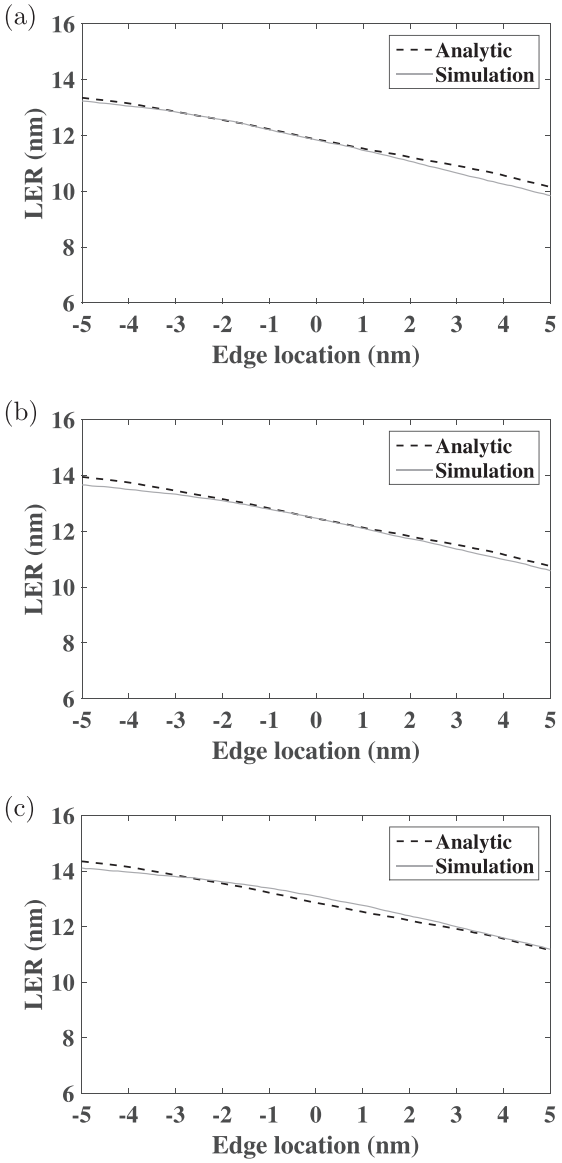

FIG. 11. LER estimated by the analytic and simulation methods at the test locations (in Fig. 12): line width of 50 nm, 500 nm PMMA on Si, beam energy of 50 keV, and dose of 64 $\mu C/cm^2$.

analytically estimated at the critical locations. Since the location dependency of LER mainly comes from the global exposure, the interpolation is done according to the spatial distribution of global exposure (see Fig. 5). In Fig. 11, the LER obtained through the interpolation is compared with the simulation result at three test locations shown in Fig. 12. The results show that the LER's estimated at the three critical locations are sufficient to accurately compute the LER at other locations through the interpolation in a large uniform pattern.

It is worthwhile to point out that the stochastic properties such as the mean and variance of developing rate used by the analytic method are obtained from the stochastic PSFs generated by the Monte Carlo simulation. That is, the same samples of developing-rate distributions are used by both the simulation and analytic methods for comparison. The simulation method measures the LER from the resist profile

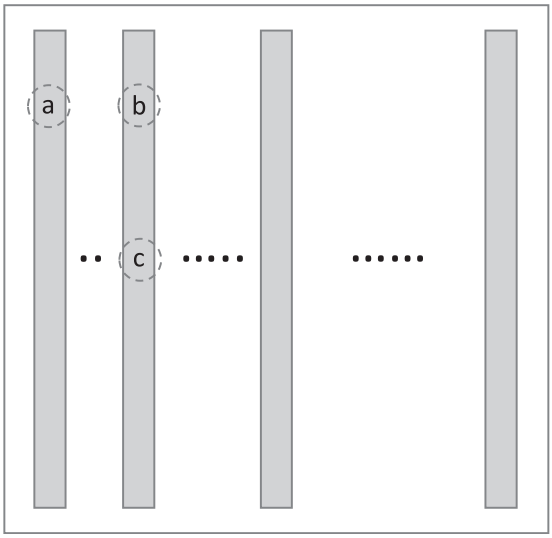

FIG. 12. Three test regions (a, b, and c) marked by circles in a large uniform pattern. Regions b and c are in the line 4μm from the left boundary of the pattern.

obtained through the development simulation. On the other hand, the analytic method computes the LER through the computational procedures, e.g., deriving the development path, the fluctuation of developing time, the direction of development path, the global exposure distribution, etc.

VI. SUMMARY

As the feature size decreases, the LER will eventually become a resolution-limiting factor in e-beam lithography, since the LER does not scale with the feature size. Therefore, it is essential to minimize the LER in order to achieve the highest resolution possible by the e-beam lithographic process. The main drawback of a simulation approach to estimating the LER is the intensive computation required. In this study, a new analytic method for estimating the LER in a large uniform pattern is developed based on the LER expression for a single line, derived in our previous study, by relating the location dependency of LER to the spatially varying global exposure.

It has been shown that the results obtained by this analytic approach for estimating the LER are closely matched with the simulation results. In this study, a uniform dose is assumed within a pattern. One of the future research items is to extend the results in this paper to allow a nonuniform dose distribution which would be needed for the proximity effect correction. Also, it will be attempted to develop an analytic method to minimize the LER and CD error by optimizing the uniform dose level or nonuniform distribution of dose in a large pattern.

ACKNOWLEDGMENT

This work was supported by a research grant from Samsung Electronics Co., Ltd.

[1]R. Rau, J. McClellan, and T. Drabik, J. Vac. Sci. Technol., B **14**, 2445 (1996).
[2]G. P. Watson, L. A. Fetter, and J. A. Liddle, J. Vac. Sci. Technol., B **15**, 2309 (1997).

[3]R. Murali, D. Brown, K. Martin, and J. Meindl, J. Vac. Sci. Technol., B **24**, 2936 (2006).
[4]Q. Dai, S.-Y. Lee, S.-H. Lee, B.-G. Kim, and H.-K. Cho, J. Vac. Sci. Technol., B **29**, 06F314 (2011).
[5]M. Nagase, H. Namatsu, K. Kurihara, K. Iwadate, K. Murase, and T. Makino, Jpn. J. Appl. Phys., Part 1 **35**, 4166 (1996).
[6]H. Eisenmann, T. Waas, and H. Hartmann, J. Vac. Sci. Technol., B **11**, 2741 (1993).
[7]S.-Y. Lee and B. D. Cook, IEEE Trans. Semicond. Manuf. **11**, 108 (1998).
[8]M. Osawa, K. Takahashi, M. Sato, and H. Arimoto, J. Vac. Sci. Technol., B **19**, 2483 (2001).
[9]Q. Dai, S.-Y. Lee, S.-H. Lee, B.-G. Kim, and H.-K. Cho, J. Vac. Sci. Technol., B **30**, 06F307 (2012).
[10]J. Bolten and T. Wahlbrink, Microelectron. Eng. **88**, 1910 (2011).
[11]W. Cho and H. Kim, J. Korean Phys. Soc. **56**, 1767 (2010).
[12]X. Zhao, S.-Y. Lee, J. Choi, S.-H. Lee, I.-K. Shin, and C.-K. Jeon, J. Vac. Sci. Technol., B **32**, 06F505 (2014).
[13]J. A. Croon, G. Storms, S. Winkelmeier, I. Pollentier, M. Ercken, S. Decoutere, W. Sansen, and H. E. Maes, *IEDM02 International Electron Devices Meeting* (2002), p. 307310.
[14]C. H. Diaz, H. Tao, Y. Ku, A. Yen, and K. Young, IEEE Electron Device Lett. **22**, 287 (2001).
[15]R. Guo, S.-Y. Lee, J. Choi, S.-H. Lee, I.-K. Shin, C.-U. Jeon, B.-G. Kim, and H.-K. Cho, J. Vac. Sci. Technol., B **33**, 06FD07 (2015).
[16]R. Guo, S.-Y. Lee, J. Choi, S.-H. Lee, I.-K. Shin, C.-U. Jeon, B.-G. Kim, and H.-K. Cho, J. Vac. Sci. Technol., B **31**, 06F408 (2013).
[17]Q. Dai, R. Guo, S.-Y. Lee, J. Choi, S.-H. Lee, I.-K. Shin, C.-U. Jeon, B.-G. Kim, and H.-K. Cho, Microelectron. Eng. **127**, 86 (2014).